ACS Catalysis

Research Article

pubs.acs.org/acscatalysis

Operando Infrared (IR) Coupled to Steady-State Isotopic Transient Kinetic Analysis (SSITKA) for Photocatalysis: Reactivity and Mechanistic Studies

Mohamad El-Roz,* Philippe Bazin, Marco Daturi, and Frederic Thibault-Starzyk

Laboratoire Catalyse et Spectrochimie, ENSICAEN, Université de Caen, CNRS, 6, boulevard du Maréchal juin, 14050 Caen, France

Supporting Information

ABSTRACT: This paper reports the coupling of operando infrared (IR) and steady-state isotopic transient kinetic analysis (SSITKA) for air purification studies from volatile organic campounds (VOCs) by photocatalysis. Methanol photo-oxidation has been used as a model reaction. A new photocatalyst (TiO_2-L) has been studied and compared to the reference material TiO_2-P25. We show that turnover frequency (TOF) values are not really available in heterogeneous photocatalysis where the number and/or efficiency of active sites can vary from one TiO_2 material to another and from one experimental setup to another. The influence of methanol concentration and reaction temperature on photocatalytic activity and on selectivity was also investigated. TiO_2-L is as active as TiO_2-P25 at low methanol concentration and is more selective at high methanol concentrations. SSITKA clarified the role of the surface formate species in the reaction mechanism. Most of these formate species are spectators and are not the main intermediates in alcohol photo-oxidation. A graduation was found in the efficiency of active sites on photocatalyst surfaces.

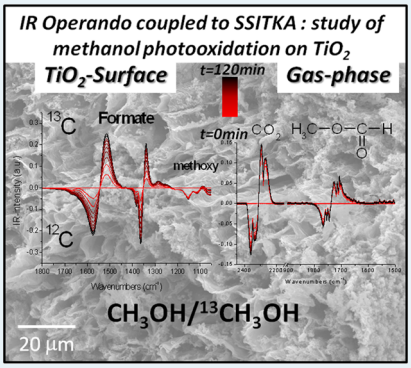

KEYWORDS: *IR-operando, SSITKA, photocatalysis, TiO_2, methanol photo-oxidation, methyl formate, CO_2 selectivity, air purification*

1. INTRODUCTION

The exponential growth of population accompanied with a high increase of industrial and military activities have caused a rapid degradation of air and water quality in the past few years. Consequently, environmental pollution is now a major global priority, requiring considerable research effort. New analytical, biochemical, and physicochemical methods are developed and studied for the characterization and elimination of hazardous chemical compounds from air, soil, and water. Advanced oxidation processes (AOPs), and especially heterogeneous photocatalysis, are intended to be both supplementary and complementary to some of the more conventional approaches to the destruction and/or transformation of hazardous chemical wastes, such as filtration,[1] anaerobic digestion,[2] and conventional physicochemical treatment.[3−6] In the field of air cleaning technologies, heterogeneous photocatalysis is a well-established and widely investigated process for the oxidation of many pollutants in air, especially indoor air where pollution can be even more important.[7,8] More than 2000 companies now commercialize different photocatalytic products, mainly for self-cleaning applications.[7−9] Therefore, the developments of new techniques and methods to investigate photocatalytic activity of solids, in water and/or air, become more and more important. During the past decade, more than 22 000 papers on photocatalysis have been published, out of which only ∼5% deal with its application to air purification, versus more than 32% for water purification.[10,11] The reasons for this could well be experimental difficulties, since studying heterogeneous photocatalysis is often more difficult in the gas phase than in the liquid phase:

(i) Contrary to water purification, where the photocatalyst can be used as a suspension, photocatalysis processes (or studies) for air purification require fixation of the photocatalyst on a support or/and on the reactor surface. In most cases, this requires the use of a binder, which could influence photocatalytic activity.
(ii) A homogeneous and reproducible irradiation of the photocatalyst surfaces is needed in order to have reproducible experiments and results.
(iii) The amount of photocatalyst used must be known accurately and the loss of material during the reaction must be kept to a minimum.
(iv) For spectroscopic studies, the design of the reactor can be difficult, and, for example, the internal volume of the reactor must be kept as small as possible to minimize the optical pathway in the gas phase and to decrease residence time.
(v) The reaction parameters (e.g., air composition, air flow (or contact time), temperature, irradiation intensity, ...) must be easily and accurately controlled, etc.

For these reasons, we have developed recently a new operando infrared (IR) reactor for studying photocatalytic

Received: July 26, 2013
Revised: September 27, 2013
Published: October 2, 2013

   dx.doi.org/10.1021/cs4006088 | ACS Catal. 2013, 3, 2790−2798

Table 1. Characteristic of TiO_2-L and TiO_2-P25 Photocatalysts Used in This Work

photocatalyst	crystallinity	morphology	BET surface area, S_{BET} (m^2/g)	mesoporous volume, V_{meso} (cm^3/g)	wavelength, λ (nm)[a]
TiO_2-L	anatase (>95%)	tubular macrofibers	90	0.14	<416
TiO_2-P25	anatase (80%), rutile (20%)	agglomerated powders	55		<405

[a]Wavelengths of the photocatalyst absorbance.

processes for air purification.[12,13] This technique presents several advantages:

(i) The photocatalyst is used and studied under the form of thin pellets, which allows limiting the mass loss, with an accurate control of the photocatalyst mass, and ensures a homogeneous irradiation of the photocatalyst surface.
(ii) The irradiation intensity can be easily controlled and the irradiation source can be changed (to monochromatic or polychromatic irradiations, UV and/or visible light sources, ...) without changing the photoreactor.
(iii) The dead volume is reduced to ~0.4 mL (residual space between each sample face and the photoreactor windows).
(iv) The reactor is coupled to online analysis techniques, such as IR gas cell and mass spectrometry (or gas chromatography−mass spectrometry (GC-MS)), which provides photocatalytic activity and selectivity data with high precision.
(v) The heating temperature of the reactor cell can be controlled from room temperature (RT) to 600 °C, and the volatile organic compounds (VOCs) or different gas concentrations can be controlled from a few ppm to a few percent. The air composition (VOCs mixture, humidity, toxic gas, ...) and the gas flow (from 1 to 50 cm^3/min) can reproduce the real conditions of the photocatalytic reaction, and the influence of these parameters on photocatalytic activities and selectivities is easily studied.

This paper demonstrates the reliability of this technique in the study of the photoactivity and selectivity of a newly elaborated TiO_2 photocatalyst (TiO_2-L) and of TiO_2-P25 (Evonik-Degussa) in the purification of air from methanol used as a model molecule for VOCs. We already previously presented the role of surface sites for the adsorption of reactants and for the formation of intermediates in RT methanol photo-oxidation.[12] The usually accepted mechanism involves formate species as main intermediates (as is the case for thermal oxidation[14]), since these formates were detected by IR spectroscopy on the surface, but no kinetic proof for the validation of this hypothesis has ever been reported.[12,15,16] For these reasons, we further investigated this system using the SSITKA approach (isotopic exchange techniques ($^{12}CH_3OH/^{13}CH_3OH$)) combined with an operando IR analysis system, which is a methodology that has already shown excellent results in methanol oxidation studies[17] but, until now, was not accessible in photocatalysis. We also report the influence of some other parameters on the CO_2 selectivity and activity of TiO_2, such as the temperature and the methanol concentration.

2. EXPERIMENTAL SECTION

2.1. Synthesis and Characterization of TiO_2-L. Hierarchical TiO_2 (TiO_2-L) has been synthesized and characterized as described in ref 18. The seeding of natural Luffa sponge (used as a biotemplate) with anatase TiO_2 was accomplished by a 24-h hydrothermal synthesis at 100 °C, under autogenous pressure. A synthesis mixture with the following composition $10Ti(OEt)_4$:$45C_2H_5OH$:$45H_2O$ (vol %) was used. The precursor solution was stirred with the Luffa sponges at RT for 1 h. Then, 100 mL of the solution (together with 500 mg of Luffa sponge) was poured into Teflon-lined stainless steel autoclaves. After the synthesis, the Luffa sponges were removed from the autoclaves, thoroughly cleaned (in order to remove the excess of TiO_2 seeds loosely bound on the substrate) with ethanol and water, and dried overnight at 60 °C. After rinsing, the samples (TiO_2/Luffa) were calcined under air, with a 5-h ramp to 500 °C and a 5-h dwell time. A macrotubular TiO_2 shape with macrochannels was obtained after removal of the natural organic support (replica of Luffa fibers) (see Figure S1 in the Supporting Information). Then, TiO_2-L samples were characterized using X-ray diffraction (XRD), N_2 sorption, and ultraviolet−visible light (UV-vis) spectroscopy;[18] the results are collected in Table 1. As a comparison, photo-oxidation was also performed on a commercial TiO_2 from Evonik-Degussa (TiO_2-P25).

2.2. Photocatalysis. The photocatalytic oxidation of methanol was performed using the new operando IR reactor described in ref 13. The TiO_2-L and TiO_2-P25 (Degussa) were pressed into self-supported wafers (Ø = 16 mm, $m \approx 10$ mg/cm^2, thickness = 50−60 μm (measured by Micromaster-IP54)). The cell was connected to gas lines with gas mixing devices and mass flow controllers. The two gas mixtures, so-called activation and reaction flows, could be prepared and sent independently to the reactor cell. Exhaust gases (reactive and/or reaction products) can be analyzed by a quadrupole mass spectrometer (Pfeiffer Omnistar GSD 301), while complementary information on the gas phase can be gained by IR spectroscopy through a gas microcell. IR spectra (64 scans per spectrum) of the catalyst under working conditions were collected at a time resolution of 1 spectrum every 2 min with a Thermo Scientific Nicolet 6700 spectrometer, equipped with a MCT detector. More details can be found in the references for both the operando IR system[19−21] and the modified IR reactor cell.[12] All IR spectra are displayed as absorbance. For this specific study, the system was equipped with two saturators in the same thermostatic bath (at exactly the same temperature), in order to send, via a four-way valve, a fixed concentration of vaporized methanol, either in its natural form or 99.0% ^{13}C enriched, provided by Cambridge Isotope Laboratories. The flow conditions were as follows: 400−1200 ppm CH_3OH, 20% oxygen in argon at a constant gas hourly space velocity of 60 000 h^{-1}. A calibration curve was drawn to establish the linear relationship between the concentration of methanol and the MS (at m/z = 29) and IR (at 1038−1026 cm^{-1}) signals (see Figure S2 in the Supporting Information). Other MS signals are also monitored in the 2−70 m/z range. In particular, m/z = 18, 33, 44, and 45 are tracked for water, $^{13}CH_3OH$, $^{12}CO_2$, and $^{13}CO_2$, respectively. The reaction was studied at RT. We have considered that the steady state of the reaction was reached

dx.doi.org/10.1021/cs4006088 | ACS Catal. 2013, 3, 2790−2798

when no more changes in both the MS signals and the IR spectra were observed (15−60 min). A monochromatic UV irradiation at 365 nm (where TiO_2-L and TiO_2-P25 present a similar absorption) with $I_0 \approx 11$ mW/cm^2 was used in order to simplify the discussion of the results. It was applied with a Xe−Hg lamp (LC8 Spot Light Hamamatsu, L10852, 200 W) and a 365-nm band-pass filter (Hamamatsu). In addition, the use of the monochromatic filter allows excluding the IR radiation of the lamp, which could increase the temperature of the pellet by a few degrees. A UV-light guide (A10014-50-0110) mounted at the entrance of a modified operando IR cell was used to establish a homogeneous irradiation, (as shown in Scheme S1 in the Supporting Information). N.B.: under polychromatic irradiation (ref 13), TiO_2 presents a higher activity and selectivity than under monochromatic irradiation. Under the same irradiation conditions, TiO_2-25 presented the same activity here as in our previous work. The methanol conversion and CO_2 selectivity were calculated as reported in our previous work.[12]

3. RESULTS AND DISCUSSION

3.1. Photocatalytic Activity and Selectivity of TiO_2-L and TiO_2-P25, and the Effect of the Methanol Concentration. In order to compare photocatalytic activity and selectivity for TiO_2-L and TiO_2-P25, the photo-oxidation of methanol was performed under the same conditions for different methanol concentrations ([MeOH]). The concentration of methanol in the gas was measured using the surface area of the MeOH-IR band at 1090−950 cm^{-1} and the MeOH-MS signal at m/z = 29 (a calibration curve is presented in Figure S2 in the Supporting Information). Selectivity for CO_2 (selectivity of the reaction for a complete methanol mineralization) was determined using the IR band area at 2395−2182 cm^{-1} and/or the MS signal at m/z = 44. Figure 1

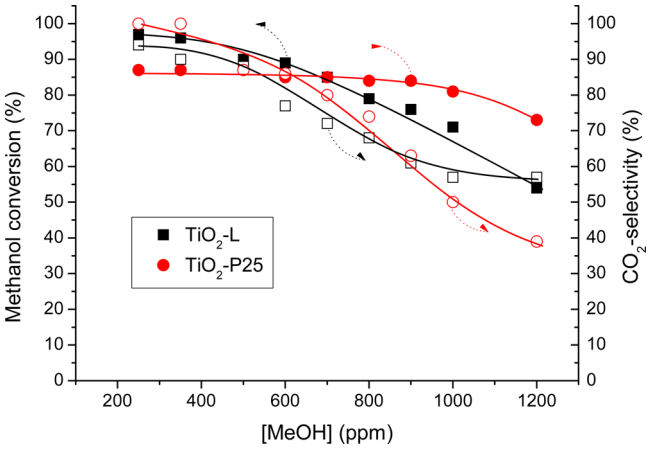

Figure 1. Influence of the methanol concentration on the methanol conversion (solid symbols) and CO_2 selectivity (open symbols) for the methanol photo-oxidation reaction using TiO_2-L (□,■) and TiO_2-P25 (○,●) photocatalysts. (Conditions: 20% O_2/Ar vol %; flow = 25 cm^3/min; RT; $I_{0(366)}$ ~10 mW/cm^2; λ = 366 nm.)

presents the evolution of methanol conversion and CO_2 selectivity versus MeOH concentration. For each concentration, methanol conversion and CO_2 selectivity were calculated after the stabilization of the gas-phase IR spectra and MS signals, i.e., irradiation time of 30−60 min after each flow modification (see Figure S3 in the Supporting Information). As reported in our previous work,[13] the methanol concentration can significantly influence the activity and the selectivity of the reaction. For a concentration lower than 600 ppm, TiO_2-L shows activity and CO_2 selectivity in the same range as TiO_2-P25 (see Figure 1). In this range of concentration, the CO_2 selectivity is slightly affected for both TiO_2-L and TiO_2-P25. For a concentration higher than 600 ppm, the methanol conversion on TiO_2-L is lower than that on TiO_2-P25. An important decrease in the CO_2-selectivity could be also observed, less pronounced on TiO_2-L than on TiO_2-P25. New IR bands at 1755 cm^{-1} and 1195 cm^{-1}, assigned, respectively, to the ν(C═O) and ν(C−O) vibration modes of methyl formate,[12] are observed in the reaction gas phase (see Figure 2). The increase of these bands (and the m/z = 60 MS

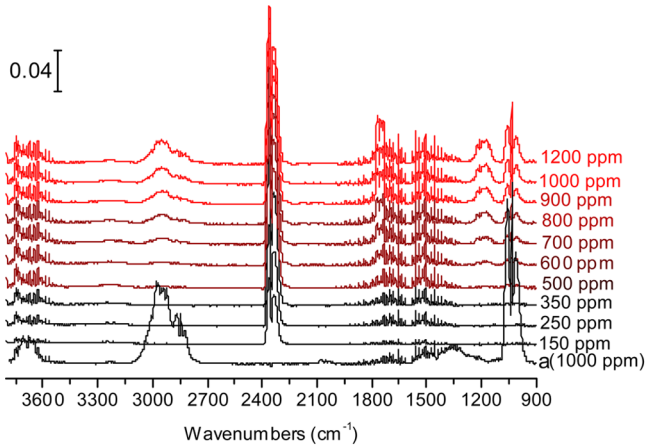

Figure 2. Original IR spectra of the gas phase during the photocatalytic reaction at RT using TiO_2-L as photocatalyst, at different methanol concentrations. "a" corresponds to the IR spectrum of 1000 ppm of methanol before photo-oxidation.

signal) with methanol concentration explains the decrease in CO_2 selectivity. The maximum amount of converted methanol (Table S1 in the Supporting Information) is ~700 ppm/min (with ~55% CO_2 selectivity) for TiO_2-L and ~800 ppm/min for TiO_2-P25 (with 50% CO_2 selectivity). Therefore, the maximum amount of "mineralized" methanol on both TiO_2-L and TiO_2-P25 is ~400 ppm/min (under the experiment conditions described in the experimental part). These results show that the increase in methanol concentration promotes the formation of methylformate by increasing the surface coverage by methanol.

The turnover frequency (TOF) is important for comparing heterogeneous catalysts.[22] As in enzymatic or homogeneous catalysis, the TOF corresponds to the number of molecules converted per second and per active site (or per catalytic molecule).[23] In heterogeneous catalysis, the TOF is often more difficult to determine, and the number of active sites can be largely unknown and is generally overestimated, considering all the theoretically calculated sites on the sample as accessible and active. In the case of solid/gas photocatalysis, it could be even worse: the actual operating surface is not known, since some parts of photocatalyst particles are not illuminated (inhomogeneous irradiation), as a consequence of internal shading.[22,24,25] In our case, the use of the photocatalyst under the form of a thin pellet (~40 μm) allows a homogeneous and reproducible illumination of the photocatalyst. On the other hand, the possibility of internal shading of the TiO_2 particles does not

dx.doi.org/10.1021/cs4006088 | ACS Catal. 2013, 3, 2790−2798

preclude the comparison between two photocatalysts where the effect will be the same. Consequently, a more-reliable estimation of the TOF will be used in this study for an additional comparison of TiO_2-L and TiO_2-P25. Practically, we used the surface density of titanol groups Ti−OH (equal to 5×10^{18} OH/m^2 or 5 OH/nm^2,[26]) as the upper limit for the number of active sites (n_{sites}). The methanol conversion rate (V_{MeOH}) corresponds to the amount of methanol converted (in milliliters, mL) per gram of photocatalyst (g^{-1}_{cat}) per minute of irradiation time (min^{-1}). The results for TOF and V_{MeOH} are presented in Figure 3, as well as in Table S1 in the Supporting Information. Conversion rates are similar for both photocatalysts, but since TiO_2-L has a higher specific surface area (Table 1), the TOF for TiO_2-L is 2−3 times lower than that for TiO_2-P25. This means that the active sites are less efficient on TiO_2-L than on TiO_2-P25 or that only a fraction of the sites are accessible or active. This overestimation of the TOF value may also well be related to electronic properties, which could be different in both photocatalysts. The hierarchical form of TiO_2-L, for example, could affect the generation of electron−hole pairs, electron−hole diffusion, trap sites, etc. In this case, TOF values calculated without taking into account these parameters would not be acceptable.

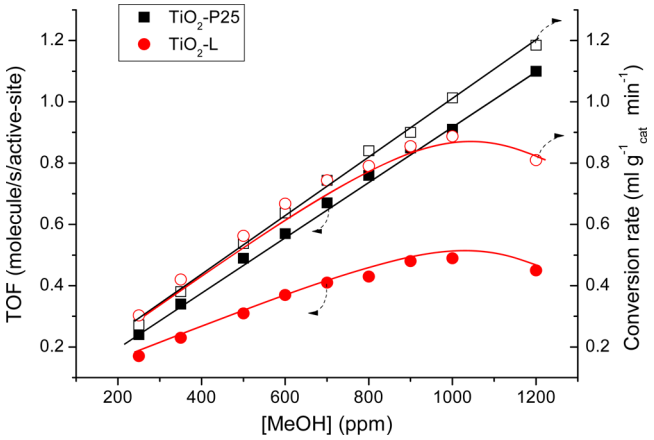

Figure 3. Influence of methanol concentration on turnover frequency (TOF) (close symbols) and on methanol conversion rate (in mL/g photocatalyst/min) (open symbol) for the methanol photo-oxidation reaction using TiO_2-P25 (square) and TiO_2-L (circle) as photocatalysts. (Conditions: 20%O_2/Ar vol %; flow = 25 cm^3/min; RT; $I_{0(366)} \approx 10$ mW/cm^2; λ = 366 nm.)

Operando IR in the photocatalytic reactor shed some more light on these reactions. During UV irradiation, new bands appeared (see Figure 4, as well as Figure S4 in the Supporting Information), assigned to monodentate and bidentate formate species adsorbed on the catalyst surface.[12,13,27,28] These species are commonly described as intermediates in the photo-oxidation of alcohols.[12,15,16,29−34] We observed different vibration bands for bidentate formates on TiO_2-L (maxima at 1600, 1373, and 1356 cm^{-1}) and on TiO_2-P25 (maxima at 1570, 1379, 1362 cm^{-1}), probably because of a difference in the nature of the formation/adsorption site. In addition, the IR intensity of these bands is much higher on TiO_2-L than on TiO_2-P25 (see Figure 4). This could be due to (i) the higher specific surface of TiO_2-L (~1.6 times higher than TiO_2-P25), leading to a greater formation of formate species, and/or (ii) a stronger adsorption of bidentate formate species on TiO_2-L than on TiO_2-P25, thus reducing their transformation.

The increase of methanol concentration led to a simultaneous increase of some corresponding IR band intensities, which was more important on TiO_2-L than on TiO_2-P25, with a maximum at 800 ppm (see Figures 5A and 5B). The same catalytic activities were observed on both photocatalysts when working in reverse concentration order, from higher to lower MeOH concentrations, which rules out surface deactivation at high methanol concentration. In addition, no deactivation was observed during the 6 h of photo-oxidation of 1200 ppm methanol on TiO_2-P25 and TiO_2-L.

These results raise the question about the alleged role of intermediates for the formates on the TiO_2 surface.

3.2. Influence of Temperature on the Activity of TiO_2-L. The influence of temperature on the activity of TiO_2-P25 has already been discussed (under polychromatic irradiation) in a previous work.[12] Results for TiO_2-L are reported in Figure 6. Both activity and selectivity increase with temperature, similar to TiO_2-P25.[12] For T > 75 °C, methanol conversion is higher than 90% (vs ~55% at RT), with complete mineralization (vs 60% CO_2 selectivity at RT). Following the formate species on TiO_2-L with temperature is easy, because of the high intensity of the corresponding IR bands (Figure 7). An important decrease is observed with increasing temperature, especially

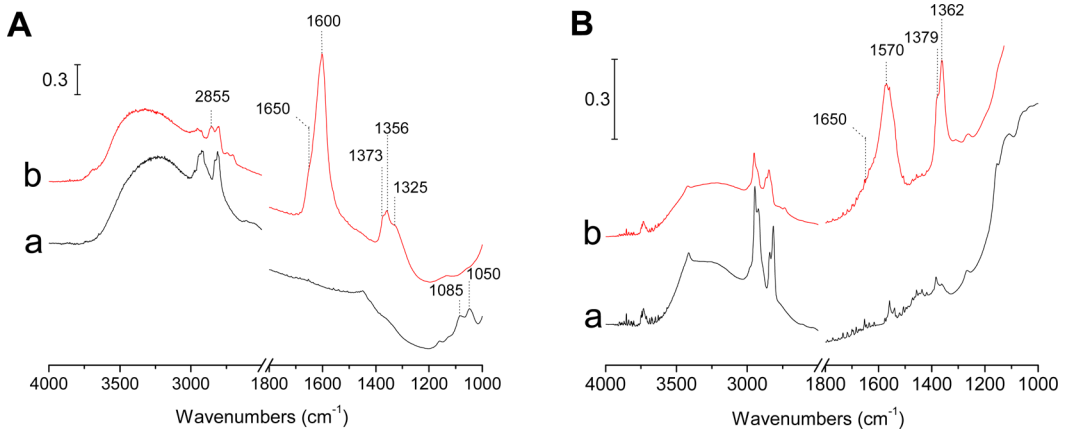

Figure 4. Infrared (IR) spectra of (A) TiO_2-L and (B) TiO_2-P25 (before (a) and after (b) 60 min of UV irradiation). The vertical scale has been amplified in panel B to ease identification of the bands. (Conditions: 1200 ppm of methanol in synthetic air; flow = 25 cm^3/min; RT; $I_{0(366)} \approx 10$ mW/cm^2; λ = 366 nm.)

dx.doi.org/10.1021/cs4006088 | ACS Catal. 2013, 3, 2790−2798

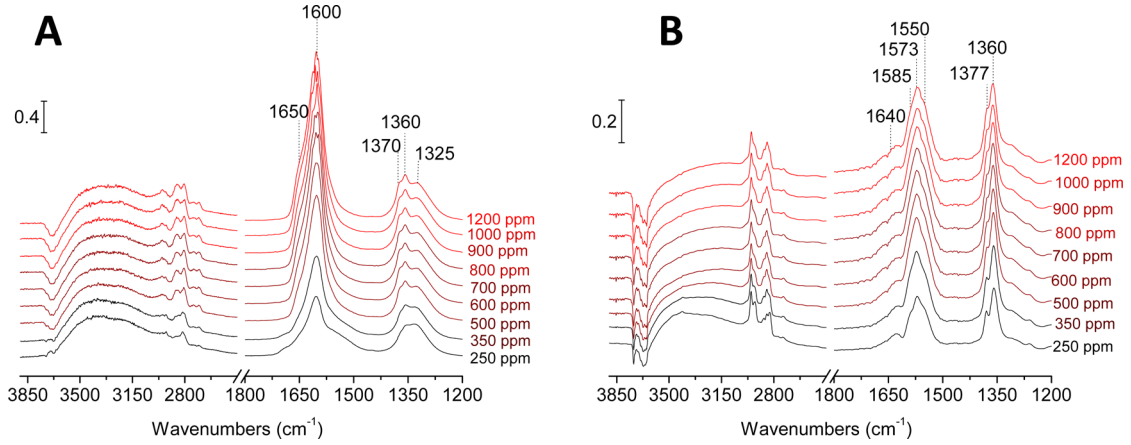

Figure 5. IR spectra of (A) TiO_2-L and (B) TiO_2-P25 after ~1 h of methanol photo-oxidation at different methanol concentrations. (Subtraction results from IR spectra recorded in darkness.)

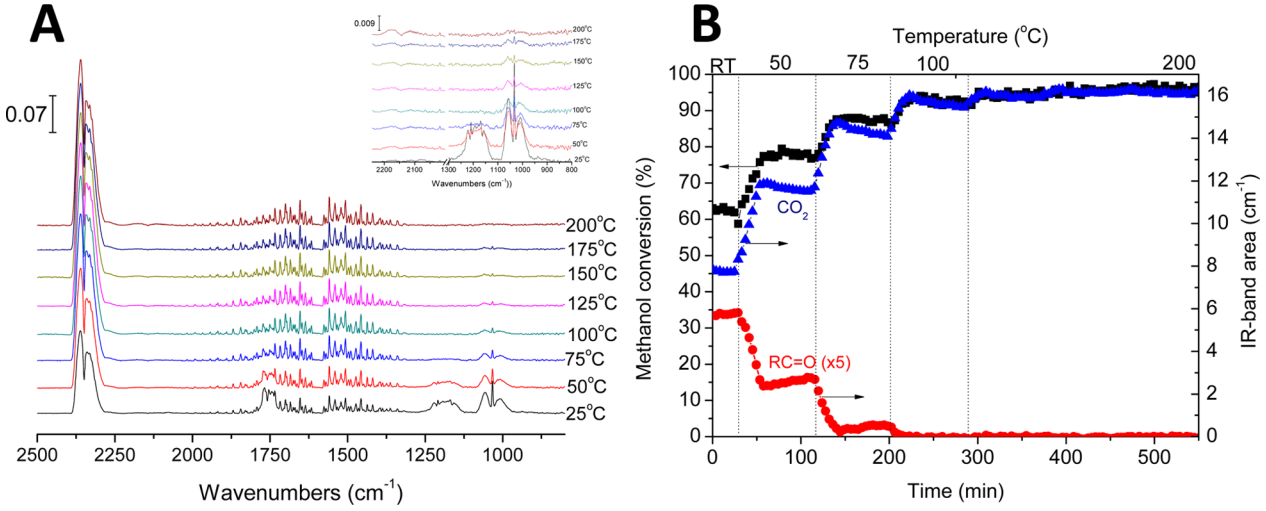

Figure 6. (A) Evolution of the gas-phase IR spectra versus reactor temperature for the methanol photo-oxidation reaction using TiO_2-L as a photocatalyst. (B) Evolution of (■) methanol conversion (calculated using the IR band at 1090−950 cm^{-1}) and the IR band areas of (▲) CO_2 (2395−2182 cm^{-1}) and (●) carbonyl species ($R_2C{=}O$; 1810−1717 cm^{-1}) at different temperatures. (Conditions: [MeOH] = 1200 ppm; $I_{0(366)} \approx$ 10 mW/cm^2; λ = 366 nm; flow = 25 cm^3/min; heating rate = 1 °C/min; and stabilization for ~1 h/temperature step.)

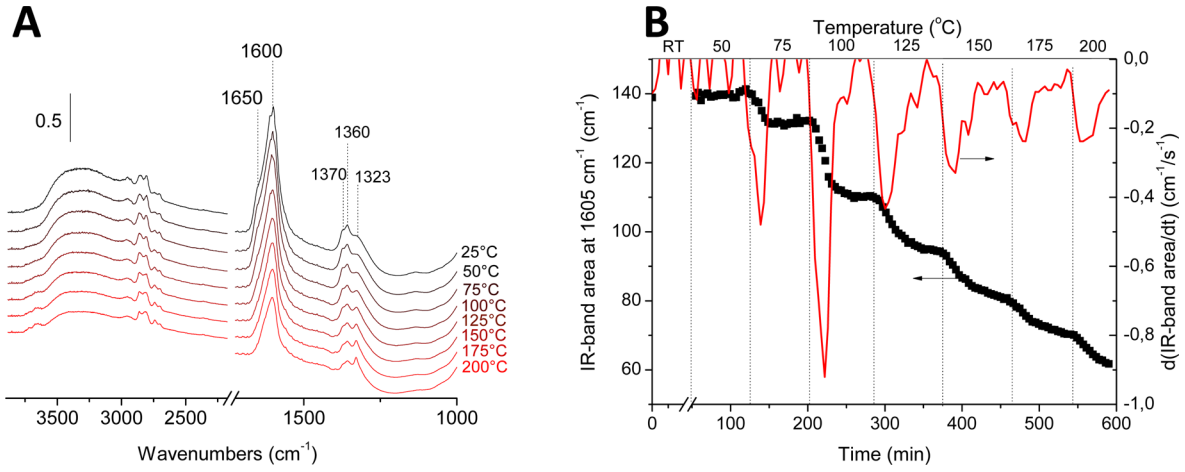

Figure 7. (A) Original IR spectra of the TiO_2-L surface at different temperatures of methanol photo-oxidation. (B) Evolution of the IR band area of formate species at 1605 cm^{-1} and their derivative versus the temperature (d(IR band area)/dT) using TiO_2-L as a photocatalyst.

between 200 °C and 240 °C, as shown by the first derivative over time of the formate band area at ~1605 cm^{-1}. This apparent decrease of surface formates with increasing temperature (and activity) already raises the question about the role of

dx.doi.org/10.1021/cs4006088 | ACS Catal. 2013, 3, 2790−2798

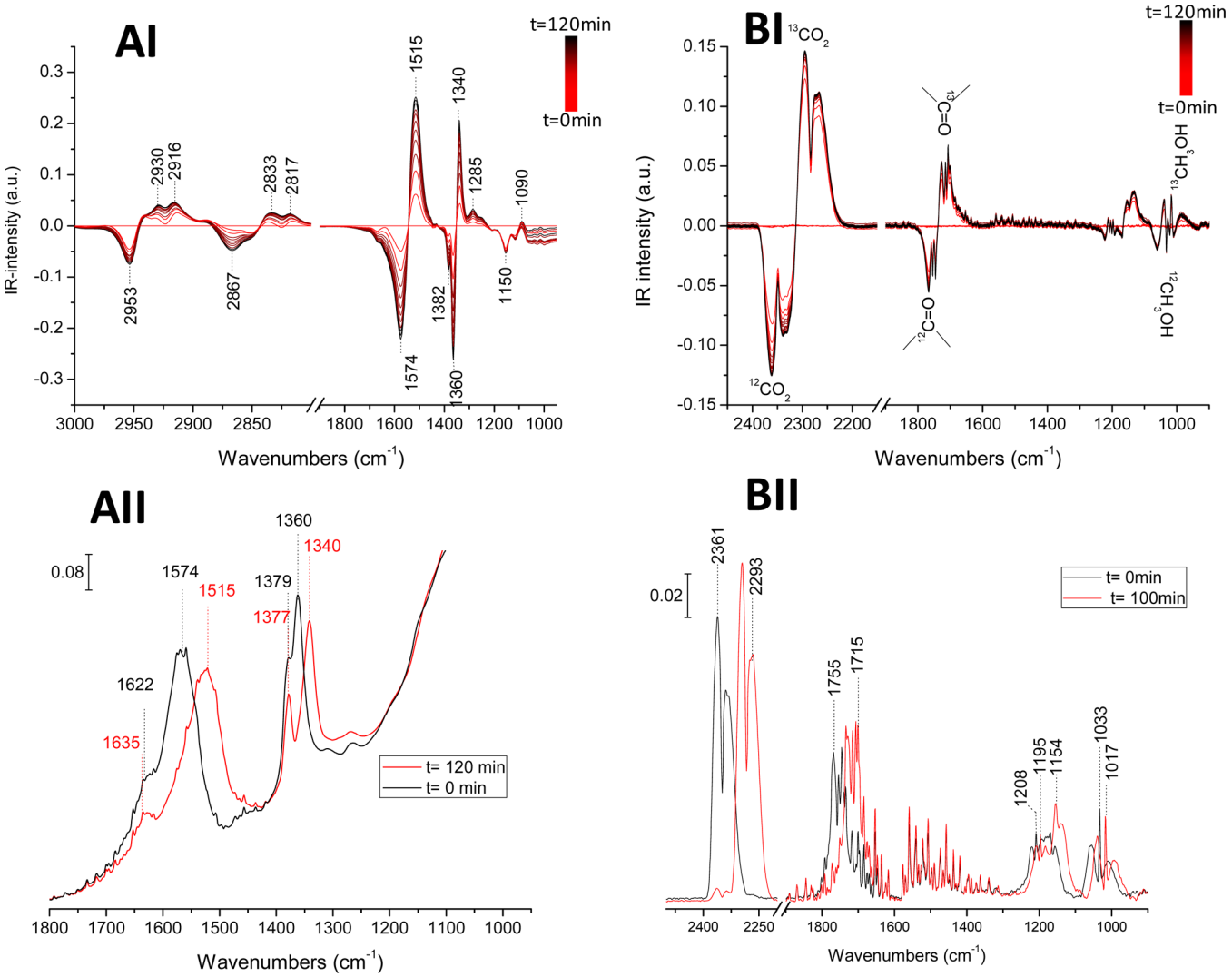

Figure 8. IR spectra of TiO_2−P25 (A) and of the reaction gas phase (B) during a SSITKA experiment for which an initial flow of 1200 ppm of $^{12}CH_3OH$, 20% of oxygen diluted in Ar (total flow =25 cm^3 min^{-1}) was switched to a similar but labeled ($^{13}CH_3OH$) flow (the spectrum recorded at t = 0 was used as background). Panels AII and BII correspond to the original IR spectra of TiO_2−P25 and of the reaction gas phase, respectively, during the SSITKA experiment at t = 0 and t = 120 min.

formates in the photocatalytic oxidation of methanol (and alcohols) and of their true intermediate nature. In addition, stationary IR bands could also be observed even at high temperature, showing the formation and presence of stable species on the photocatalyst during photo-oxidation.

3.3. Role of Formate Species in Methanol Photo-oxidation: A Complementary Study by SSITKA. SSITKA is a methodology for obtaining transient conditions while remaining under the required chemical and/or kinetic steady-state environment for a given reaction. It is already used in some operando studies for a better understanding or clarification of the mechanism of a catalytic reaction, and sometimes to determine the activation energy.[35−40] In our case, SSITKA experiments were performed to clarify the role of formate species in methanol photo-oxidation. Two reaction flow lines in our operando system have been used; each is equipped with a saturator containing either natural or ^{13}C-enriched methanol (recall Scheme S1 in the Supporting Information). A four-way valve allows instantaneous switching from one flow to another under the same experimental conditions (flow = 25 cm^3/min, concentration = 1200 ppm, temperature = RT, UV irradiation intensity $I_{0(366)} \approx 11$ mW/cm^2; λ = 366 nm; and air composition = 20% oxygen in argon), and the reaction remains chemically identical in both cases. The chosen methanol concentration led to incomplete conversion and partial mineralization of methanol (Figure 1), which allowed the following isotopic exchange of all species, including reactants with the online gas analyses. The switch from ^{12}C- to ^{13}C-substituted methanol was done during the photo-oxidation reaction and the switching time used was t = 0. The exchange of formates on TiO_2-L is very slow, and only 50% of the formates were exchanged after more than 350 min (~6 h). The results presented here were obtained on TiO_2−P25, and those with TiO_2-L are presented in the Supporting Information.

Starting from the chemical steady state (t = 0), the reaction flow was switched from natural to labeled methanol. Consequently, the bands of adsorbed ^{13}C-methoxy (1090 cm^{-1}) and ^{13}C-formates (1340 and 1515 cm^{-1}) species progressively replaced those of the unlabeled species (see Figure 8AI), giving rise to several isosbestic points. On the time traces (Figure 9A), crossing points are observed at $t \approx 5$ min and $t \approx 18$ min (>75 min for TiO_2-L; see Figure S5 in the

dx.doi.org/10.1021/cs4006088 | ACS Catal. 2013, 3, 2790−2798

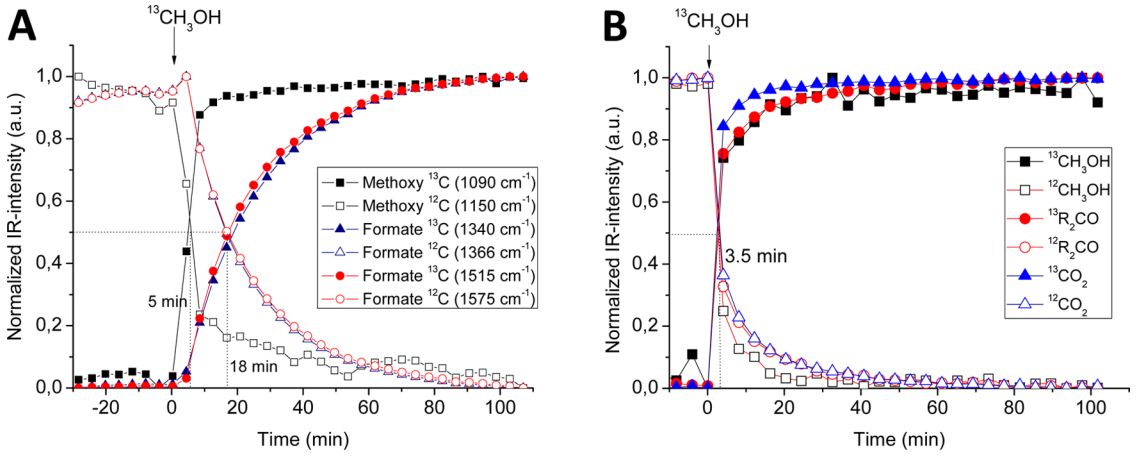

Figure 9. Evolution of the IR band intensities (A) for adsorbed species on TiO_2-P25 and (B) for final products detected in the gas phase, each versus irradiation time.

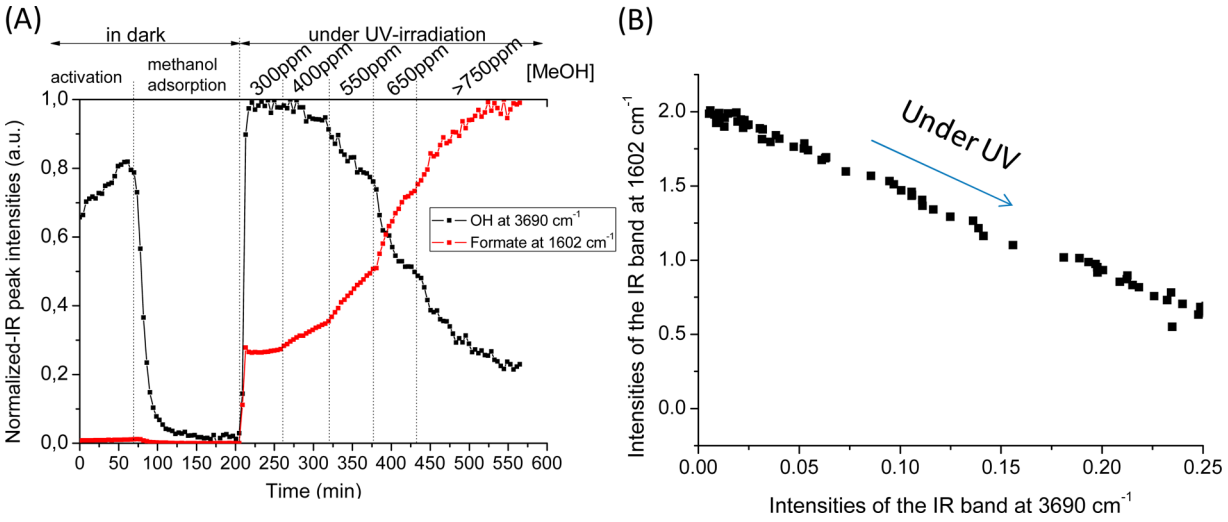

Figure 10. (A) Evolution of the IR band of TiOH at 3690 cm^{-1} and of formate species at 1602 cm^{-1} during methanol photo-oxidation. (B) Evolution of the formate species IR-band vs Ti(III)OH IR-band during methanol photo-oxidation.

Supporting Information) for adsorbed methoxy and formate species, respectively. The online analyses of the exhaust gases show similar isosbestic and crossing points (at $t \approx 3.7$) for methanol, carbon dioxide, and carbonyl compounds (methyl formate with traces of formaldehyde and/or formic acid) (see Figures 8BI and 9B, as well as Figure S5 in the Supporting Information). Similar results were obtained on TiO_2-L (see Figure S4 in the Supporting Information). The kinetic behavior of surface methoxy groups is coherent with the kinetics of the changes in the reactor exhaust, but formate species are clearly reacting too slowly, compared to the speed of CO_2 and methyl formate productions. These results show that the majority of formate species formed on the TiO_2 surface are spectators. Only a part of these formates are the real intermediates in methanol photo-oxidation. The rate difference between the exchange of the surface formates and the exchange of the final products is explained by different conversion rates for different formates on the surface, and by a graduation in the activity of different active sites. This conclusion is in agreement with the relatively lower activity founded on TiO_2-L, at high methanol concentration, despite the higher amount of formate species observed on the surface of this material (compared to TiO_2-P25). In addition, adsorbed methoxy groups, which present an isotopic exchange rate similar to the exchange rate of final products, could rather be effective and be the first intermediates in methanol photo-oxidation.

However, even after a complete replacement of $^{13}CH_3OH$ by $^{12}CH_3OH$ in the gas phase (after $t = 8$ min; see Figure S6 in the Supporting Information), traces of $^{12}CO_2$ could still be observed at $t = 360$ min, because of the slow decomposition of unlabeled surface formates. Therefore, two reaction pathways exist on the surface for the photocatalytic oxidation of methanol: a fast (and major) one, and a side path, via the slow decomposition of surface formates. The fast reaction could go via some of the formates (could be the formates formed on the surface exposed directly to the light) or via surface carbonates, but no carbonate bands were detected. A slower rate for the isotopic exchange of surface formates was observed on TiO_2-L (crossing point at $t > 75$ min vs 18 min for TiO_2-P25). Switching to pure air, with zero methanol concentration, under UV irradiation, does not change the rate for formates removal from the surface. In addition, persistent IR bands were detected on the photocatalysts after isotopic exchange, because of stable formates formed on the surface after irradiation (in agreement with the observed influence of temperature).

dx.doi.org/10.1021/cs4006088 | ACS Catal. 2013, 3, 2790−2798

IR spectra for TiOH groups on the surface during the photocatalytic process give information on the possible sites for the formation of weakly or not active formate species (see Figure 10). The evolution of the IR spectra of TiO_2 in real time is presented in Figure S7 in the Supporting Information. Methanol adsorption led to the perturbation of surface TiOH groups and to the total disappearance of the IR bands at 3720 cm^{-1} and 3690 cm^{-1} assigned to the stretches of two different hydroxyls (see Figure S4 in the Supporting Information). After irradiation, the lower wavenumber band was recovered while the other remained perturbed (see Figure S8 in the Supporting Information). Figure 10B shows the linear relationship between the IR bands of the surface formate species and that of the band at 3720 cm^{-1}. This shows the function of the role that TiOH plays in the stabilization of the formate on the photocatalyst surface. The higher band intensity for formates on TiO_2-L is thus due to a larger amount of TiOH sites on the surface of the solid. It should be noted that the higher absorption in the visible-light region for TiO_2-L is probably linked to the presence of oxygen vacancies, resulting in an absorbance red-shift (see Table 1).

4. CONCLUSION

The new operando-IR technique presented here shows high performance to highlight the activity of the photocatalyst, the selectivity of the reaction, and the role of the surface species in the reaction mechanism. However, in situ identification of the species formed on the photocatalyst surface is not enough to determine their role in the reaction. We used the new technique to study the activity and selectivity of a new photocatalyst (TiO_2-L), with methanol photo-oxidation as a model reaction for air purification from volatile organic campounds (VOCs). TiO_2-P25 (Evonik-Degussa) was used as reference under the same reaction conditions. TiO_2-L presents a higher activity at low methanol concentration and higher selectivity at high methanol concentration, compared to TiO_2-P25. The turnover frequency (TOF) of the reaction was calculated using a theoretical number of active site in anatase TiO_2. It is 2−3 times lower in the case of TiO_2-L than for TiO_2-P25. This was assigned to an overestimation of the number of active sites in TiO_2-L and showed that the real number is lower than estimated. A similar methanol conversion rate (expressed in units of mL $g_{TiO_2}^{-1}$ min^{-1}) was found for both photocatalysts. The photo-oxidation activity and CO_2 selectivity of TiO_2 increase with temperature. Formate species are formed and adsorbed in higher amounts on TiO_2-L than on TiO_2-P25. A 40 cm^{-1} shift could be also observed between the IR spectra of TiO_2-P25 and TiO_2-L surfaces. Steady-state isotopic transient kinetic analysis (SSITKA) experiments allowed relationships to be established between surface species and final products. Formates formed on TiO_2-L are more stable than on TiO_2-P25. Of the entire population of formate species on the surface, only a minor part are involved in the reaction, and the major portion are only spectator species. A relationship between the formation of stable formates and the disappearing of hydroxyls was also observed, showing the role of defects and TiOH sites in the stabilization of low active formate on the surface. During SSITKA experiments, the exchange rates for methoxy and final products were the same on both photocatalysts, suggesting methoxy as the first intermediates in methanol photooxidation. Operando IR is thus demonstrated as an important technique in photocatalysis, unveiling more information than other, sometimes more-expensive, techniques. In the future, operando IR will be coupled with SSITKA using different methanol isotopes ($CH_3{}^{18}OH$ and CD_3OH) in order to determine the real intermediates and global mechanism in methanol photo-oxidation.

■ ASSOCIATED CONTENT

Supporting Information

This material is available free of charge via the Internet at http://pubs.acs.org.

■ AUTHOR INFORMATION

Corresponding Author

*E-mail: mohamad.elroz@ensicaen.fr.

Notes

The authors declare no competing financial interest.

■ REFERENCES

(1) Athanasekou, C. P.; Romanos, G. E.; Katsaros, F. K.; Kordatos, K. V.; Likodimos; Falaras, P. *J. Membr. Sci.* **2012**, *392*, 192−203.
(2) Maroga Mboulaa, V.; Hequeta, V.; Grub, Y.; Colinb, R.; Andresa, Y. *J. Hazard. Mater.* **2012**, *209*, 355−364.
(3) Wilsonb, D.; Wangb, W.; Lopesa, R. J. G. *Appl. Catal. B* **2012**, *123*, 273−281.
(4) Konstantinou, I. K.; Albanis, T. A. *Appl. Catal. B* **2004**, *49*, 1−14.
(5) Gogate, P. R.; Pandit, A. B *Adv. Environ. Res.* **2004**, *8*, 501−551.
(6) Galindo, C.; Jacques, P.; Kalt, A. *J. Photochem. Photobiol. A: Chem.* **2000**, *130*, 35−47.
(7) Fujishima, A.; Zhangb, X.; Tryk, D. A. *Surf. Sci. Rep.* **2008**, *63*, 515−582.
(8) Fujishima, A.; Zhangb, X. *C. R. Chim.* **2006**, *9*, 750−760.
(9) Ganesh, V. A.; Kumar Raut, H.; Nair, A. S.; Ramakrishna, S. *J. Mater. Chem.* **2011**, *21*, 16304−16322.
(10) *Web of Knowledge*; Thomson Reuters: New York, http://wokinfo.com, 2013.
(11) *Scifinder*; Chemical Abstracts Service: Columbus, OH, https://scifinder.cas.org, 2013.
(12) El-Roz, M.; Kus, M.; Cool, P.; Thibault-Starzyk, F. *J. Phys. Chem. C* **2012**, *116*, 13252−13263.
(13) El-Roz, M.; Bazin, P.; Thibault-Starzyk, F. *Catal. Today* **2013**, *205*, 111−119.
(14) Rousseau, S.; Marie, O.; Bazin, P.; Daturi, M.; Verdier, S.; Harlé, V. *J. Am. Chem. Soc.* **2010**, *132*, 10832−10841.
(15) Sun, S.; Ding, J.; Bao, J.; Gao, C.; Qi, Z.; Li, C. *Catal. Lett.* **2010**, *137*, 239−246.
(16) Panayotov, D. A.; Burrows, S. P.; Morris, J. R. *J. Phys. Chem. C* **2012**, *116*, 6623−6635.
(17) Bazin, P.; Thomas, S.; Marie, O.; Daturi, M. *Catal. Today* **2012**, *182*, 3−11.
(18) El-Roz, M.; Haidar, Z.; Al-Lakiss, L.; Toufaily, J.; Thibault-Starzyk, F. *RCS Adv.* **2013**, *3*, 3438−3445.
(19) Lesage, T.; Verrier, C.; Bazin, P.; Saussey, J.; Daturi, M. *Phys. Chem. Chem. Phys.* **2003**, *5*, 4435−4440.
(20) Malpartida, I.; Ivanova, E.; Mihaylov, M.; Hadjiivanov, K.; Blasin-Aubé, V.; Marie, O.; Daturi, M. *Catal. Today* **2010**, *149*, 295−303.
(21) Wuttke, S.; Bazin, P.; Vimont, A.; Serre, C.; Seo, Y.-K.; Hwang, Y. K.; Chang, J.-S.; Férey, G.; Daturi, M. *Chem.—Eur. J.* **2012**, *18*, 11959−11967.
(22) Herrmann, J.-M. *J. Photochem. Photobiol. A: Chem.* **2010**, *216*, 85−89.
(23) Boudart, M. ; Djéga-Mariadassou, G. *Cinétique des réactions en catalyse hétérogène*; Masson: Paris, 1982.
(24) Parmon, V.; Emeline, A. V.; Serpone, N. *Int. J. Photoenergy* **2002**, *4*, 91−131.

(25) Braslavsky, S. E.; Braun, A. M.; Cassano, A. E.; Emeline, A. V.; Litter, M. I.; Palmisano, L.; Parmon, V. N.; Serpone, N. *Pure Appl. Chem.* **2011**, *83*, 931−1014.
(26) Boehm, H. P. *Adv. Catal.* **1966**, *16*, 179−274.
(27) Chuang, C. C.; Wu, W. C.; Huang, M. C.; Huang, I. C.; Lin, J. L. *J. Catal.* **1999**, *185*, 423−434.
(28) Popova, G. Y.; Andrushkevich, T. V.; Chesalov, Y. A.; Stoyanov, E. S. *Kinet. Catal.* **2000**, *41*, 805−811.
(29) Hernandez-Alonso, M.; Tejedor-Tejedor, I.; Coronado, J. M.; Anderson, M. A. *Appl. Catal. B* **2011**, *101*, 283−293.
(30) Arana, J.; Dona-Rodriguez, J. M.; Cabo, C. G. i; Gonzalez-Diaz, O.; Herrera-Melian, J. A.; Perez-Pena, J. *Appl. Catal. B* **2004**, *53*, 221−232.
(31) Kominami, H.; Sugahara, H.; Hashimoto, K. *Catal. Commun.* **2010**, *11*, 426−429.
(32) Coronado, J. M.; Kataoka, S.; Tejedor-Tejedor, I.; Anderson, M. A. *J. Catal.* **2003**, *219*, 219−230.
(33) ven der Meulen, T.; Mattson, A.; Osterlund, L. *J. Catal.* **2007**, *251*, 131−144.
(34) Guzman, F.; Chuang, S. S.C. *J. Am. Chem. Soc.* **2010**, *132*, 1502−1503.
(35) Bazin, P.; Thomas, S.; Marie, O.; Daturi, M. *Catal. Today* **2012**, *182*, 3−11.
(36) Efstathiou, A. M.; Verykios, X. E. *Appl. Catal. A* **1997**, *151*, 109−166.
(37) Olympiou, G. G.; Kalamaras, C. M.; Zeinalipour-Yazdi, C. D.; Efstathiou, A. M. *Catal. Today* **2007**, *127*, 304−318.
(38) Meunier, F. C.; Reid, D.; Goguet, A.; Shekhtman, S.; Hardacre, C.; Burch, R.; Deng, W.; Flytzani-Stephanopoulos, M. *J. Catal.* **2007**, *247*, 277−287.
(39) Wang, J.; Kispersky, V. F.; Delgass, W. N.; Ribeiro, F. H. *J. Catal.* **2012**, *289*, 171−178.
(40) Shannon, S. L.; Goodwin, J. G. *Chem. Rev.* **1995**, *95*, 677−695.